Published in final edited form as:
Bone. 2012 September ; 51(3): 459–465. doi:10.1016/j.bone.2012.05.023.

Mechanotransduction in bone tissue: The A214V and G171V mutations in Lrp5 enhance load-induced osteogenesis in a surface-selective manner☆

Paul J. Niziolek[a,b], **Matthew L. Warman**[c,d], and **Alexander G. Robling**[a,e,*]

[a]Department of Anatomy & Cell Biology, Indiana University School of Medicine, Indianapolis, IN, USA

[b]Weldon School of Biomedical Engineering, Purdue University, West Lafayette, IN, USA

[c]Department of Orthopaedic Surgery, Children's Hospital, Boston, MA, USA

[d]Howard Hughes Medical Institute, Department of Genetics, Harvard Medical School, Boston, MA, USA

[e]Department of Biomedical Engineering, Indiana University-Purdue University at Indianapolis (IUPUI), Indianapolis, IN, USA

Abstract

Mechanotransduction in bone requires components of the Wnt signaling pathway to produce structurally adapted bone elements. In particular, the Wnt co-receptor LDL-receptor-related protein 5 (LRP5) appears to be a crucial protein in the mechanotransduction cascades that translate physical tissue deformation into new bone formation. Recently discovered missense mutations in LRP5 are associated with high bone mass (HBM), and the altered function of these proteins provide insight into LRP5 function in many skeletal processes, including mechanotransduction. We further investigated the role of LRP5 in bone cell mechanotransduction by applying mechanical stimulation in vivo to two different mutant mouse lines, which harbor HBM-causing missense mutations in Lrp5. Axial tibia loading was applied to mature male Lrp5 G171V and Lrp5 A214V knock-in mice, and to their wild type controls. Fluorochrome labeling revealed that 3 days of loading resulted in a significantly enhanced periosteal response in the A214V knock in mice, whereas the G171V mice exhibited a lowered osteogenic threshold on the endocortical surface. In summary, our data further highlight the importance of Lrp5 in bone cell mechanotransduction, and indicate that the HBM-causing mutations in Lrp5 can alter the anabolic response to mechanical stimulation in favor of increased bone gain.

Keywords

Wnt; Lrp5; HBM; Loading; Mechanotransduction; Osteoporosis

☆This work was supported by NIH grant AR53237 (to AGR), and by the Howard Hughes Medical Institute (to MLW).

*Corresponding author at: Department of Anatomy & Cell Biology, Indiana University School of Medicine, 635 Barnhill Dr., MS 5035, Indianapolis, IN 46202, USA. Fax: +1 317 278 2040. arobling@iupui.edu. .

Introduction

Mechanical loading of bone induces adaptive changes in the bone structure and geometry, achieved by altered bone resorption and formation activity [1,2]. In vivo experiments in rodents show that exogenous mechanical loading of bone tissue leads to increased transcription of WNT/β-catenin responsive genes and reporter molecules in osteocytes, and that unloading of bone leads to decreased WNT/β-catenin signaling due to increased sclerostin expression [3–5]. These results have been confirmed in vitro, where cultured bone cells express WNT/β-catenin responsive genes in response to mechanical stimulation [4,6]. An important component of the WNT/β-catenin signaling pathway in bone is the low density lipoprotein receptor-related protein 5 (LRP5), a WNT co-receptor that plays a major role in bone mass regulation in humans and mice [7–11].

Beyond its general role in bone metabolism, LRP5 is necessary for load induced bone formation. We previously reported that Lrp5 knock-out mice have an almost complete ablation of the anabolic response to mechanical loading of the ulna, compared to wild-type (WT) relatives [12]. These effects have been confirmed in another, independently generated Lrp5 knockout mouse, using a different loading model [13]. Moreover, clinical data also support the role of LRP5 signaling in regulating bone mechanotransduction. In a large human sample, Kiel et al. reported that several single nucleotide polymorphisms (SNPs) in LRP5, located in exons 10 and 18, significantly affected the relation between physical activity and bone mass accrual [14]. Collectively, these observations indicate that LRP5 is a critical component of the mechanical signaling cascade in bone.

Certain missense mutations near the N-terminus of LRP5 have been reported to cause a high bone mass (HBM) phenotype in humans [8,9,15,16]. In vitro experiments in cell lines transfected with LRP5 HBM mutations revealed that the mutation confers resistance to the endogenous Lrp5 antagonists, Dkk1 [8,17,18] and sclerostin [19–23]. The observed resistance to these and other Lrp5 inhibitors might be the mechanism by which the HBM phenotype emerges in humans and mice.

Several years ago, a mouse model for the LRP5 HBM phenotype was generated using a transgenic overexpression approach. Those mice harbor a transgene coding for the human LRP5 G171V HBM mutation, driven by a 3.6 kb fragment of the rat ColIαI promoter [7]. This mouse strain exhibits significantly increased bone mineral density, similar to that seen in humans. Overall, the mice have higher bone structural strength (ultimate force, yield force, and stiffness) and apparent material properties (ultimate stress, yield stress, and flexural modulus) [24]. This mouse was also reported to have an increased sensitivity to load, due to a lower threshold for initiating bone formation [4,13]. More recently, we reported the development of two Lrp5 HBM mouse models, in which we have knocked-in the G171V or A214V missense mutations into the endogenous Lrp5 sequence [25,26]. These mice express the HBM mutant receptors at normal levels and in normal (naturally occurring) tissues, due to retention of the endogenous Lrp5 promoter driving transcription. Similar to the HBM patients, we have found that both knock-in mouse lines have a strong HBM phenotype.

The non-invasive rodent axial tibial-loading model has been developed to apply a controlled mechanical load to the tibia through the knee and ankle joints [27,28]. This model presents an alternative to the ulnar loading model, which directly applies a load to the ulna at the proximal end. Because the axial tibia loading model applies force to the tibia through the proximal and distal joint surfaces, the loading environment might more closely approximate the physiological application of load.

In the present communication, we investigated the cortical bone formation response in Lrp5 G171V and A214V knock-in and wild-type (WT) mice, after application of an equivalent mechanical stimulus using the non-invasive tibial-loading model. We hypothesized that both HBM-causing mutations would result in larger load-induced bone formation parameters compared to the WT mice. We found that A214V mice had significantly greater periosteal bone formation compared to WT at the proximal and midshaft locations of the tibia. However, periosteal bone formation at all sites in G171V mice was not significantly greater than was observed in WT mice. On the endocortical surface, we observed a significant load-induced upregulation of bone formation only in the G171V mice, indicating that G171V mice may have a lower strain threshold for bone formation. In summary, our data further highlight the importance of Lrp5 in bone cell mechanotransduction, and indicate that the HBM-causing mutations in Lrp5 can alter the anabolic response to mechanical stimulation in favor of increased bone gain.

Materials and methods

Animals

Generation of knock-in mice with the A214V and G171V mutations in Lrp5 has been described previously [25]. Briefly, two targeting constructs spanning introns 2–4 were generated, which harbored the G171V or A214V mutation located in exon 3. The constructs were introduced into mouse embryonic stem (ES) cells, and standard selection techniques were used to identify clones in which the construct properly recombined into the endogenous Lrp5 sequence. The ES cells were implanted into pseudopregnant females, and chimeric pups were identified and bred using standard techniques. The mice were bred to homozygosity ($Lrp5^{+/+}$ [designated as WT], $Lrp5^{A214V/A214V}$ [designated as Lrp5 A214V], or $Lrp5^{G171V/G171V}$ [designated as Lrp5 G171V]). The genetic background of all mice was a uniform mixture of 129S1/SvIMJ and C57Bl/6J. All animal procedures performed in accordance with guidelines set by the Indiana University Institutional Animal Care and Use Committee.

Strain gage measurements

Four 18 week-old male mice homozygous for one of the three Lrp5 genotypes (WT, A214V, G171V) were sacrificed and right hindlimb was frozen at −20 °C until strain gage testing. Limbs were allowed to warm to room temperature over several hours and muscle tissue was carefully dissected away to reveal the midshaft tibia. A strain gage (EA-06-015DJ-120, Vishay) was applied to midshaft of tibia on the posterior surface (surface between tibia and fibula) and the tibia was placed into the loading cups (Figs. 1A and B). We determined the microstrain:load ratio for each sample using progressively increasing load applications while simultaneously recording the voltage output from the load cell and strain gage. All tests were averaged within each genotype to determine the microstrain:load ratio for each genotype. A peak microstrain value of 2120 was chosen to be applied to all genotypes and this corresponded to peak loads of 9.0, 14.4, and 9.8 N for WT, A214V, G171V genotypes, respectively (Fig. 1A).

Loading protocol

At 18 weeks of age, 8 male mice of each Lrp5 genotype (WT, A214V, G171V) began the axial tibia loading protocol. Mice were anesthetized using isoflurane inhalation, and their right hindlimb (knee to foot) was placed in molded loading cups that secured the tibia (Fig. 1B). A sinusoidal wave form (2 Hz, 120 cycles) was applied with a peak load as described above. Mice were given three bouts with a day of rest between each bout. Intraperitoneal injection of alizarin was given 1 day after the final bout followed by an intraperitoneal injection of calcein 8 days later. Mice were sacrificed 17 days after the final bout. The right

and left tibias were harvested and placed in 10% NBF for 2 days followed by storage in 70% ethanol at 4 °C.

Histological processing and measurements

Tibias were dehydrated in graded alcohols, cleared in xylene, and embedded in methylmethacrylate following standard protocols. Thick-cut sections were taken at locations 25% (proximal), 50% (midshaft), and 75% (distal) of total tibia length and ground down to ~30 μm. A single unstained section from each tibia was digitally imaged on a fluorescent microscope using filter sets that provide excitation and emission for the calcein and alizarin wavelengths (Fig. 2). Digital images were imported into ImagePro Express (Media Cybernetics, Inc., Gaithersburg, MD) and the following histomorphometric measurements were recorded for the endosteal and periosteal surfaces: total perimeter, single label perimeter (sL.Pm), double label area and perimeter, total bone area and marrow area. The following results were calculated: double label perimeter (dL.Pm=double label circumference/2), mineral apposition rate (MAR=double label area/dL.Pm/8 days), mineralizing surface (MS/BS=(0.5×sL.Pm+dL.Pm)/total perimeter×100), and bone formation rate (BFR/BS=MAR×MS/BS×3.65).

Statistical methods

Measurements comparing right (loaded) vs left (non-loaded) bones were analyzed for statistical significance using a paired student's *t*-test. Measurements comparing genotypes used relative values, calculated by subtracting the nonloaded (left leg) values from the loaded (right leg) values, to account for differences within a mouse. Student's *t*-test was used to compare Lrp5 HBM mice to WT mice. Significance was taken at $p<0.05$.

Results

Control limb bone formation parameters are similar among Lrp5 WT, A214V, and G171V mice at 20 wks of age

To assess baseline bone formation rates among the three Lrp5 genotypes, left (nonloaded) tibial bone formation parameters were measured and compared. Mineral apposition rates (MAR), mineralizing surface (MS/BS), and bone formation rates (BFR/BS) were similar among all three genotypes, for both endocortical and periosteal surfaces and at all three diaphyseal locations, with one exception (Table 1). The only parameter that was significantly affected by genotype was periosteal MS/BS at the proximal diaphyseal location. Post-hoc tests revealed that the Lrp5 G214V mice had significantly reduced ($p=0.02$) proximal tibia periosteal MS/BS, compared to WT mice.

Mechanical loading increases periosteal bone formation in the tibia, and Lrp5 A214V mice have an increased load-induced periosteal bone formation response compared to WT mice

The axial tibia loading model induced a significant increase in periosteal bone formation in the loaded limb compared to non-loaded limb in all three genotypes examined (Table 1). However, this effect was observed only for the proximal and midshaft locations, but not at the distal location (with the exception of increased periosteal MAR in the A214V mice). Comparison of the loading response in HBM mice to that measured for WT mice was facilitated by calculating relative (r) bone formation parameters for each mouse; i.e., subtracting the loaded (right) limb parameters from the corresponding non-loaded (left) limb to account for baseline differences within an animal. Compared to WT mice, A214V mice had significantly increased MAR, MS/BS, and BFR/BS at the proximal site, and significantly increased MAR and BFR/BS at the midshaft, but no significant differences from WT at the distal site (Fig. 3). Relative periosteal bone formation parameters among the

G171V mice were not significantly different from those measured in the WT mice, at all three diaphyseal locations.

Lrp5 G171V mice require less strain to activate load-induced endocortical bone formation

In WT mice, we were unable to detect a significant increase in bone formation parameters on the endocortical surface of the loaded tibiae compared to the same surface in the control tibiae. A similar lack of load-responsiveness was found on the endocortical surface of A214V tibiae. However, the loaded limbs from G171V mice had significantly increased endocortical bone formation parameters at the midshaft location compared to the non-loaded limb (Table 1). It is unclear whether this effect existed at the proximal site in these mice as we were not able to reasonably measure the endosteal surface at the proximal location due to trabeculae disrupting the majority of the endosteal surface in the HBM mice. The increased load-induced bone formation rates on the endocortical surface of G171V mice, but not of WT mice, suggest that less strain was required to activate bone formation in these mice, i.e., a lower strain threshold for the endocortical surface appears to exist in the G171V mice.

Discussion

We investigated whether the Lrp5 HBM-causing missense mutations A214V and G171V, when expressed at naturally-occurring levels and in physiologically routine cell types, confer enhanced bone formation responsiveness to mechanical loading. Our broader goal was to shed some light on whether enhanced osteo-anabolic responsiveness to everyday loading events (e.g., locomotion, physical activity) might explain a portion of the mechanisms that induce the HBM phenotype. We found that while both HBM mutations improved mechanotransduction beyond the efficiency observed in WT mice, the A214V and G171V exerted their effects on this process differently. The A214V mutation, but not the G171V mutation, was associated with an enhanced response to mechanical loading on the periosteal surface, when compared to WT mice. On the endosteal surface, we observed that the G171V mutation, but not the A214V mutation or the WT allele, conferred increased bone formation in response to loading, suggesting that the strain threshold for endocortical bone formation was lowered by the G171V mutation.

Load induced bone formation was observed in two of the three locations along the tibial diaphysis. The distal site (75%) was not responsive to mechanical loading among any of the mouse genotypes, with the exception of periosteal MAR in the A214V mice. These findings suggest that the tibia axial loading model imposes an insufficient amount of strain to this site to reliably induce bone formation. Alternatively, the lack of bone curvature in the distal diaphysis, and the consequent lack of bending that would be expected from an axial load, might account for the non-responsiveness. In support of this explanation, the proximal site that we analyzed (25%) was equally distant from the closest joint surface as was the distal site, yet the curvature is much greater in the proximal end, and the proximal site responded robustly to the loading stimulus whereas the distal site did not. Others have also reported reduced or non-significant loading effects at the distal tibia using the tibia axial loading model [28,29].

We have previously shown that a reduction in sclerostin expression is temporally and spatially associated with mechanical strain magnitude, indicating that a loss of sclerostin-mediated Lrp5 suppression might play a role in the cellular signaling cascade that leads to load-induced bone formation [30]. This hypothesis is further strengthened by our recent ulnar loading experiments in ^{8kb}Dmp1:: hSOST transgenic mice (an 8 kb fragment of the Dentin matrix protein 1 (Dmp1) promoter driving expression of human SOST), which exhibit a severe loss of mechanotransduction, similar to Lrp5 knockout mice [31]. Presumably, these mice have increased expression/release of Lrp5 agonists (e.g., Wnt

molecules), but the unrepressed transgenic expression of sclerostin prevents Wnt signaling through Lrp5. In vitro, it has been shown that several Lrp5 HBM mutations are resistant to Dkk1 and sclerostin binding [17,19,32]. Thus, if (1) HBM mutations confer immunity to sclerostin-mediated inhibition, and (2) loss of sclerostin is the sole determinant of whether mechanotransduction will occur, then we would expect to find equal bone formation in the loaded and non-loaded limbs of our HBM knock-in mice. In other words, the knock-in mice would be experiencing a constant mechanical loading signal in all bones, since they would not be inhibited by sclerostin (similar to removing sclerostin as a result of loading in WT mice). Because we observed load-induced bone gain in the knock-ins, our data indicate that mechanotransduction through the Lrp5 receptor requires not only the removal of Lrp5 inhibition, but also the upregulation/secretion of ligand(s) for enhanced receptor activation, i.e., release of Wnts or other Lrp5 agonists. Thus, the signaling mechanisms can be thought of as a two-arm process: reduction of Lrp5 inhibitors and enhancement of Lrp5 activators. If either arm is compromised, it is likely that mechanotransduction will be compromised.

Published data on the Lrp5 G171V transgenic mouse ($^{3.6kb}$ColIαI::G171V) report an enhancement in mechanical loading responsiveness through a lowered threshold for bone formation [24,33]. Our Lrp5 G171V knock-in mice had a significant load-induced response on the endocortical surface, but the same amount of mechanical strain applied to WT mice did not elicit an endocortical response. Thus, our results support the previously advanced hypothesis that the Lrp5 G171V mutation lowers the mechanical strain threshold for bone formation. Furthermore, we have reported that our two Lrp5 HBM mutant mice have a different phenotype from one another, with G171V mice preferentially adding more bone endosteally to result in a smaller medullary area than WT mice, and the A214V preferentially adding more bone periosteally to result in a larger total cross section than WT mice [26]. In that study, we observed no difference in non-loaded limb marrow area in G171V compared to WT, but A214V had an increased marrow area compared to wild type. Given the thicker cortices and smaller marrow space of the G171V mice, we calculated the strains on the endocortical surface to be ~15% lower than those calculated for WT mice (data not shown). Despite these lower strains, the G171V mice were responsive to tibial loading, whereas WT mice were not.

On the periosteal surface, we did not observe an enhanced bone formation response in the G171V compared to WT mice, which differs from Akhter et al.'s report of an enhanced periosteal formation surface response per unit strain for the G171V transgenic mice [24]. This difference might be due to their use of two different values of peak strain; the same peak load was applied to both genotypes, instead of using different loads to apply the same peak strain as we did in this experiment [33]. Moreover, the loading models employed were different; we used the axial tibial model, which produces axial compression and bending, whereas Akhter et al. used the 4-point bending model, which produces a nearly pure bending moment in the tibial midshaft. A more likely explanation, however, is the difference in receptor expression between the two models. The $^{3.6kb}$ColIαI::G171V mouse has much higher levels of receptor expression than WT mouse. In fact, overexpression of WT LRP5 ($^{3.6kb}$ColIαI::LRP5), at levels similar to those found in the high-expressing $^{3.6kb}$ColIαI::G171V line, resulted in significantly increased bone mass. Those data suggest that receptor number, independent of its mutation state, can bone mass significantly. However, the much more robust phenotype of the $^{3.6kb}$ColIαI::G171V transgenics indicates that the HBM mutation has a much more dramatic effect on bone mass than the WT allele. Nonetheless, it is unclear if the $^{3.6kb}$ColIαI::LRP5 mice would have enhanced responsiveness to loading. Secondly, the $^{3.6kb}$ColIαI promoter fragment directs HBM overexpression to a specific population of cells, which might not normally express the receptor. This might explain their periosteal phenotype, whereas our G171V phenotype was largely endocortical. Further, the $^{3.6kb}$ColIαI::G171V mice overexpress the HBM gene with

concurrent expression of endogenous Lrp5, both of which would be expected to be activated (perhaps differently) upon loading. Our HBM knock-in mice do not express any WT Lrp5 so they are not affected by this issue. A more recent publication using compressive axial loading of the tibia in the same G171V overexpresser mouse model as used by Akhter et al., reported that the $^{3.6kb}$ColIαI::G171V transgene significantly enhanced loading effects on the endocortical surface (as measured by load-induced change in medullary area) but not on the periosteal surface (as measured by load-induced change in total area) [13]. This surface-specific loading result for the G171V transgenic model is similar to that found in our G171V knock-in model. Interestingly, Saxon et al. found a sex-specific tibial loading effect for Lrp5 knockout mice, where the male Lrp5 knockouts showed no response to loading but the female knockouts were difficult to interpret [13]. One of the limitations of the present study is that we examined load-induced bone formation only in males; thus we are unable to address sex-specific effects of the knock-in alleles in mechanotransduction.

It should be noted that we also measured proximal tibia trabecular bone formation rates via fluorochrome histomorphometry (using the same pair of labels used for the cortical rates), and also static parameters of the proximal tibia trabecular meshwork (e.g., BV/TV, Tb.N) via μCT, but neither of these analyses produced a significant loading effect in the mice (data not shown). This observation is not unexpected since (1) our 3-day loading schedule was designed for histomorphometric detection of bone formation rate changes and not for more dramatic changes needed for detection by μCT, and (2) the labeling schedule employed was designed to capture the more slow-growing cortical bone, rather than the more rapidly accumulating trabecular bone in the proximal tibia.

In conclusion, we found that the bone formation response to mechanical loading was surface-specific, depending on the Lrp5 alleles present. For all Lrp5 genotypes, we found a significant increase in bone formation parameters between the loaded and non-loaded limbs on the periosteal surface. However, the A214V mutation, but not G171V, was associated with an enhanced periosteal response to mechanical loading at the proximal and midshaft tibial locations, compared to WT. Conversely, only the G171V mice achieved a significant increase in bone formation on the endosteal surface at the midshaft, suggesting a lowered threshold for bone formation in these mice. These results support the pivotal role of Lrp5 in bone mechanotransduction, and suggest that although both mutations generate a high bone mass phenotype, there may be differences in the actual mechanism that governs their achievement of this HBM phenotype.

References

[1]. Robling AG, Hinant FM, Burr DB, Turner CH. Improved bone structure and strength after long-term mechanical loading is greatest if loading is separated into short bouts. J Bone Miner Res. 2002; 17(8):1545–54. [PubMed: 12162508]

[2]. Warden SJ, Turner CH. Mechanotransduction in the cortical bone is most efficient at loading frequencies of 5-10 Hz. Bone. 2004; 34(2):261–70. [PubMed: 14962804]

[3]. Lin C, Jiang X, Dai Z, Guo X, Weng T, Wang J, et al. Sclerostin mediates bone response to mechanical unloading through antagonizing Wnt/beta-catenin signaling. J Bone Miner Res. 2009; 24(10):1651–61. [PubMed: 19419300]

[4]. Robinson JA, Chatterjee-Kishore M, Yaworsky PJ, Cullen DM, Zhao WG, Li C, et al. Wnt/beta-catenin signaling is a normal physiological response to mechanical loading in bone. J Biol Chem. 2006; 281(42):31720–8. [PubMed: 16908522]

[5]. Bonewald LF, Johnson ML. Osteocytes, mechanosensing and Wnt signaling. Bone. 2008; 42(4): 606–15. [PubMed: 18280232]

[6]. Hens JR, Wilson KM, Dann P, Chen XS, Horowitz MC, Wysolmerski JJ. TOPGAL mice show that the canonical Wnt signaling pathway is active during bone development and growth and is

activated by mechanical loading in vitro. J Bone Miner Res. 2005; 20(7):1103–13. [PubMed: 15940363]

[7]. Babij P, Zhao W, Small C, Kharode Y, Yaworsky PJ, Bouxsein ML, et al. High bone mass in mice expressing a mutant LRP5 gene. J Bone Miner Res. 2003; 18(6):960–74. [PubMed: 12817748]

[8]. Boyden LM, Mao JH, Belsky J, Mitzner L, Farhi A, Mitnick MA, et al. High bone density due to a mutation in LDL-receptor-related protein 5. N Engl J Med. 2002; 346(20):1513–21. [PubMed: 12015390]

[9]. Little RD, Carulli JP, Del Mastro RG, Dupuis J, Osborne M, Folz C, et al. A mutation in the LDL receptor-related protein 5 gene results in the autosomal dominant high-bone-mass trait. Am J Hum Genet. 2002; 70(1):11–9. [PubMed: 11741193]

[10]. Ai MR, Heeger S, Bartels CF, Schelling DK. Clinical and molecular findings in osteoporosis-pseudoglioma syndrome. Am J Hum Genet. 2005; 77(5):741–53. [PubMed: 16252235]

[11]. Gong Y, Slee RB, Fukai N, Rawadi G, Roman-Roman S, Reginato AM, et al. LDL receptor-related protein 5 (LRP5) affects bone accrual and eye development. Cell. 2001; 107(4):513–23. [PubMed: 11719191]

[12]. Sawakami K, Robling AG, Ai M, Pitner ND, Liu D, Warden SJ, et al. The Wnt co-receptor LRP5 is essential for skeletal mechanotransduction but not for the anabolic bone response to parathyroid hormone treatment. J Biol Chem. 2006; 281(33):23698–711. [PubMed: 16790443]

[13]. Saxon LK, Jackson BF, Sugiyama T, Lanyon LE, Price JS. Analysis of multiple bone responses to graded strains above functional levels, and to disuse, in mice in vivo show that the human Lrp5 G171V High Bone Mass mutation increases the osteogenic response to loading but that lack of Lrp5 activity reduces it. Bone. 2011; 49(2):184–93. [PubMed: 21419885]

[14]. Kiel DP, Ferrari SL, Cupples LA, Karasik D, Manen D, Imamovic A, et al. Genetic variation at the low-density lipoprotein receptor-related protein 5 (LRP5) locus modulates Wnt signaling and the relationship of physical activity with bone mineral density in men. Bone. 2007; 40(3):587–96. [PubMed: 17137849]

[15]. Johnson ML, Gong G, Kimberling W, Recker SM, Kimmel DB, Recker RB. Linkage of a gene causing high bone mass to human chromosome 11 (11q12-13). Am J Hum Genet. 1997; 60(6): 1326–32. [PubMed: 9199553]

[16]. Van Wesenbeeck L, Cleiren E, Gram J, Beals RK, Benichou O, Scopelliti D, et al. Six novel missense mutations in the LDL receptor-related protein 5 (LRP5) gene in different conditions with an increased bone density. Am J Hum Genet. 2003; 72(3):763–71. [PubMed: 12579474]

[17]. Ai M, Holmen SL, Van Hul W, Williams BO, Warman ML. Reduced affinity to and inhibition by DKK1 form a common mechanism by which high bone mass-associated missense mutations in LRP5 affect canonical Wnt signaling. Mol Cell Biol. 2005; 25(12):4946–55. [PubMed: 15923613]

[18]. Bhat BM, Allen KM, Liu W, Graham J, Morales A, Anisowicz A, et al. Structure-based mutation analysis shows the importance of LRP5 beta-propeller 1 in modulating Dkk1-mediated inhibition of Wnt signaling. Gene. 2007; 391(1–2):103–12. [PubMed: 17276019]

[19]. Balemans W, Piters E, Cleiren E, Ai M, Van Wesenbeeck L, Warman ML, et al. The binding between sclerostin and LRP5 is altered by DKK1 and by high-bone mass LRP5 mutations. Calcif Tissue Int. 2008; 82(6):445–53. [PubMed: 18521528]

[20]. Ellies DL, Viviano B, McCarthy J, Rey JP, Itasaki N, Saunders S, et al. Bone density ligand, Sclerostin, directly interacts with LRP5 but not LRP5G171V to modulate Wnt activity. J Bone Miner Res. 2006; 21(11):1738–49. [PubMed: 17002572]

[21]. Li X, Zhang Y, Kang H, Liu W, Liu P, Zhang J, et al. Sclerostin binds to LRP5/6 and antagonizes canonical Wnt signaling. J Biol Chem. 2005; 280(20):19883–7. [PubMed: 15778503]

[22]. Semenov M, Tamai K, He X. SOST is a ligand for LRP5/LRP6 and a Wnt signaling inhibitor. J Biol Chem. 2005; 280(29):26770–5. [PubMed: 15908424]

[23]. Semenov MV, He X. LRP5 mutations linked to high bone mass diseases cause reduced LRP5 binding and inhibition by SOST. J Biol Chem. 2006; 281(50):38276–84. [PubMed: 17052975]

[24]. Akhter MP, Wells DJ, Short SJ, Cullen DM, Johnson ML, Haynatzki GR, et al. Bone biomechanical properties in LRP5 mutant mice. Bone. 2004; 35(1):162–9. [PubMed: 15207752]

[25]. Cui Y, Niziolek PJ, MacDonald BT, Zylstra CR, Alenina N, Robinson DR, et al. Lrp5 functions in bone to regulate bone mass. Nat Med. 2011; 17(6):684–91. [PubMed: 21602802]

[26]. Niziolek PJ, Farmer TL, Cui Y, Turner CH, Warman ML, Robling AG. High-bone-mass-producing mutations in the Wnt signaling pathway result in distinct skeletal phenotypes. Bone. 2011; 49(5):1010–9. [PubMed: 21855668]

[27]. De Souza RL, Matsuura M, Eckstein F, Rawlinson SC, Lanyon LE, Pitsillides AA. Non-invasive axial loading of mouse tibiae increases cortical bone formation and modifies trabecular organization: a new model to study cortical and cancellous compartments in a single loaded element. Bone. 2005; 37(6):810–8. [PubMed: 16198164]

[28]. Fritton JC, Myers ER, Wright TM, van der Meulen MC. Loading induces site-specific increases in mineral content assessed by microcomputed tomography of the mouse tibia. Bone. 2005; 36(6):1030–8. [PubMed: 15878316]

[29]. Fritton JC, Myers ER, Wright TM, van der Meulen MC. Bone mass is preserved and cancellous architecture altered due to cyclic loading of the mouse tibia after orchidectomy. J Bone Miner Res. 2008; 23(5):663–71. [PubMed: 18433300]

[30]. Robling AG, Niziolek PJ, Baldridge LA, Condon KW, Allen MR, Alam I, et al. Mechanical stimulation of bone in vivo reduces osteocyte expression of Sost/sclerostin. J Biol Chem. 2008; 283(9):5866–75. [PubMed: 18089564]

[31]. Tu X, Rhee Y, Condon K, Bivi N, Allen MR, Dwyer D, et al. Sost downregulation and local Wnt signaling are required for the osteogenic response to mechanical loading. Bone. 2011

[32]. Balemans W, Devogelaer JP, Cleiren E, Piters E, Caussin E, Van Hul W. Novel LRP5 missense mutation in a patient with a high bone mass phenotype results in decreased DKK1-mediated inhibition of Wnt signaling. J Bone Miner Res. 2007; 22(5):708–16. [PubMed: 17295608]

[33]. Cullen DM, Akhter MP, Mace D, Johnson ML, Babij P, Recker RR. Bone sensitivity to mechanical loads with the Lrp5 HBM mutation. J Bone Miner Res. 2002; 17:S332–S332.

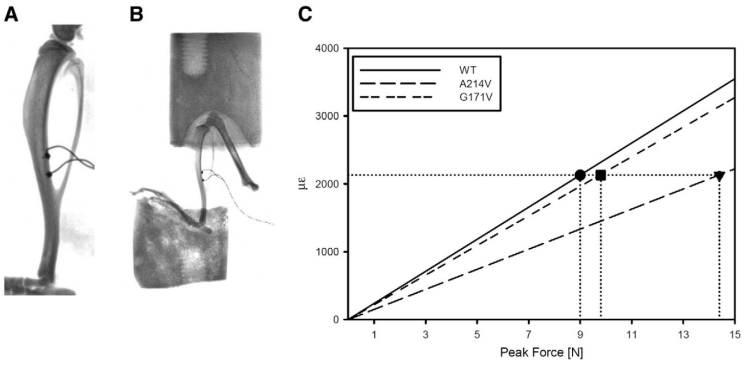

Fig. 1.

A) X-ray of excised tibia with strain gage attached at the posterior midshaft (surface between tibia and fibula). Gages were placed on 4 specimens for each Lrp5 genotype (WT, A214V, G171V) and each specimen was tested 1–4 times to determine the microstrain (με) to compressive force ratio. B) X-ray of excised lower limb in loading cups. C) The με:force ratio for the tibial midshaft as determined from strain gage testing. A peak value of 2120 με was chosen to apply to the three genotypes in the tibia loading experiment. This peak strain corresponded to a peak force of 9.0 N, 9.8 N, and 14.4 N in the WT, G171V, and A214V mice, respectively.

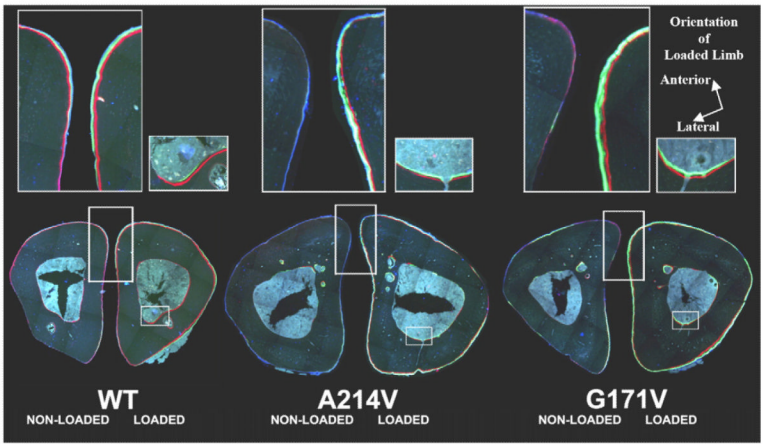

Fig. 2.

Mosaic images of non-loaded (left) and loaded (right) midshaft tibias for WT, A214V, and G171V mice. Upper panels magnify (300%) the respective areas highlighted below them (left: periosteal surface; right: endosteal surface).

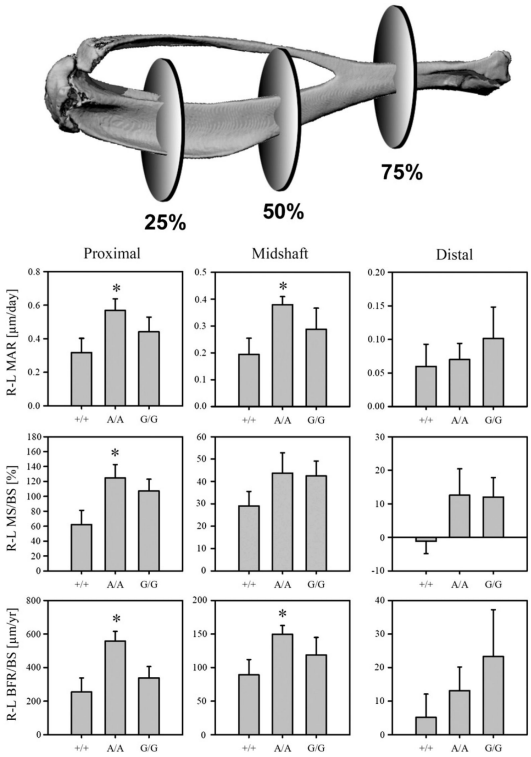

Fig. 3.

On the periosteal surface, the Lrp5 A214V mutation conferred enhanced bone formation compared to WT mice. R–L (loaded–non-loaded limb) bone formation parameters indicate that at the proximal location (25% of length along tibial axis) the A214V mutation conferred an enhanced response to mineral apposition rate (MAR), mineralizing surface (MS/BS), and bone formation rate (BFR/BS) when compared to WT mice. At the midshaft, R–L MAR and R–L BFR/BS were both significantly enhanced by the A214V mutation. No differences in response were observed at the distal location (75% along tibial axis) nor for the G171V mutation at any periosteal location. *=$p<0.05$ vs WT student's *t*-test, n=7–8 per group.

Table 1

Summary of tibial dynamic histomorphometric parameters from right and left limbs, at periosteal and endocortical surfaces, and at three diaphyseal locations.

Region Surface Lrp5 genotype Side	MAR (μm/day)	MS/BS (%)	BFR/BS ($\mu m^3/\mu m^2/yr$)
Proximal location			
Periosteal surface			
WT			
Right (loaded)	0.30±0.06	80±11	94±22
Left (control)	0.62±0.07*	143±21*	349±86*
A214V			
Right (loaded)	0.35±0.03	67±14	88±23
Left (control)	0.91±0.05*	192±9*	646±54*
G171V			
Right (loaded)	0.26±0.07	36±7	43±13
Left (control)	0.70±0.05*	143±18*	381±69*
Midshaft location			
Periosteal surface			
WT			
Right (loaded)	0.29±0.04	50±7	57±14
Left (control)	0.48±0.05*	79±7*	146±23*
A214V			
Right (loaded)	0.21±0.04	45±9	42±16
Left (control)	0.59±0.05*	88±3*	192±20*
G171V			
Right (loaded)	0.23±0.05	35±6	32±6
Left (control)	0.51±0.06*	77±5*	151±27*
Endocortical surface			
WT			
Right (loaded)	0.36±0.05	36±10	50±17
Left (control)	0.44±0.07	49±7	90±23
A214V			
Right (loaded)	0.35±0.07	29±5	40±9
Left (control)	0.45±0.05	32±5	52±10
G171V			
Right (loaded)	0.27±0.06	28±4	30±11
Left (control)	0.45±0.04*	48±6*	83±15*
Distal location			
Periosteal surface			

Region Surface Lrp5 genotype Side	MAR (μm/day)	MS/BS (%)	BFR/BS ($\mu m^3/\mu m^2/yr$)
WT			
Right (loaded)	0.16±0.06	43±8	35±17
Left (control)	0.22±0.05	42±7	40±14
A214V			
Right (loaded)	0.19±0.06	34±13	43±23
Left (control)	0.26±0.06*	47±9	56±19
G171V			
Right (loaded)	0.08±0.03	13±5	7±4
Left (control)	0.18±0.06	25±10	31±1
Endocortical surface			
WT			
Right (loaded)	0.37±0.03	38±5	54±9
Left (control)	0.46±0.04	36±4	61±9
A214V			
Right (loaded)	0.28±0.07	47±5	53±15
Left (control)	0.37±0.08	43±9	73±20
G171V			
Right (loaded)	0.16±0.08	31±15	48±29
Left (control)	0.26±0.07	41±11	57±23

Mean±standard error are reported.

* $p<0.05$ paired *t*-test nonloaded (left) vs loaded (right) limb.